Progress in Fractional Differentiation and Applications
An International Journal

http://dx.doi.org/10.12785/pfda/010205

Fractional Modeling of Typical Stages in HIV Epidemics with Drug-Resistance

Carla M. A. Pinto[1,*] *and Ana R. M. Carvalho*[2]

[1]School of Engineering, Polytechnic of Porto, Center for Mathematics of the University of Porto, Rua Dr António Bernardino de Almeida, 431, 4200-072 Porto, Portugal
[2] Faculty of Sciences, University of Porto, Rua do Campo Alegre s/n, 4440-452 Porto, Portugal

Received: 1 Jan. 2015, Revised: 23 Feb. 2015, Accepted: 27 Feb. 2015
Published online: 1 Apr. 2015

Abstract: In this paper it is studied a fractional order model for the three stages of HIV epidemics with drug-resistance. The model includes $CD4^+$ T cells, CTLs, macrophages, and the virus populations. We simulate the model for different values of the fractional derivative $\alpha \in [0.5, 1.0]$. The fractional order system untangles generous dynamical characteristics, such as faster transients and slower evolutions as time increases. These traits are not seen in integer-order models, since they are customary of memory-preserving systems.

Keywords: HIV, helper cells, macrophages, CTL, treatment, drug-resistance

1 Introduction

AIDS is a deadly disease in untreated patients. In these cases, time since initial infection till death is approximately 9-10 years. The virus responsible for the development of AIDS is the human immunodeficiency virus (HIV). HIV is a retrovirus that impairs the immune response system, by targeting the $CD4^+$ helper T cells, macrophages and dendritic cells. The cytotoxic lymphocytes (CTLs) or immune response cells, are the cells set out to eliminate infection by killing infected cells.

A typical HIV infection is, in the absence of treatment, characterized by three stages [1]. The first is the acute phase, where there is a spike in HIV load and a sharp decrease in the $CD4^+$ T cells count. Patients in this stage suffer commonly from fever, headaches, rash, pharyngitis. The second stage is the chronic phase, characterized by a dramatic drop in the viral load, approaching a quasi-steady state, and an increase in the CD4 cells' count. This behavior is explained by the balance between virus production and clearance rates [2]. After the chronic phase, AIDS takes place. In the later, the number of $CD4^+$ T cells declines steadily and the viral load increases rapidly.

Treatment for HIV/AIDS consists in the administration of antiretroviral drugs (ART) that suppress HIV viral load below the limit of detection ($\sim$50 copies/*ml*). The most common ART classes are the reverse transcriptase inhibitors (RTI), the protease inhibitors (PI), the fusion/entry inhibitors (FEI), the integrase inhibitors (II), and the multidrug inhibitors (MI). Drug-resistance is associated to high virus replication and mutation rates, poor adherence to therapy, or poor absorption and pharmacokinetics [3].

In the last few decades, scientists have devoted a considerable amount of their research time to the understanding of HIV epidemics, namely, the immune response to HIV, host/virus interaction, and the efficacy of ART regimens. Perelson *et al* [4] study a model for viral load data, collected from infected patients, after administration of a PI. They calculate the lifespan of productively infected cells and of plasma virions, the virions production rate, and the HIV-1 generation time (namely, the intracellular delay from the time virions are released until they infect another cell, and cause the release of new viruses). Hadjandreou *et al* [5], propose a model for long term HIV dynamics, subjected to continuous and structured treatment interruptions (STI). Their results show that an optimized scheduling, where the interplay between the two virus strains (drug-resistant and drug-susceptible) is facilitated, favors better responses from the patients. Optimized STI is thus promising in patients that have developed strong drug-resistance, and for whom

* Corresponding author e-mail: cap@isep.ipp.pt

continuous therapy fails. Hernandez-Vargas and Middleton [6] develop a model for the three stages of HIV infection. They conclude that macrophage population plays a key role in the progression to AIDS. Pinto and Carvalho [7] study a model for HIV dynamics in HIV-specific CD4$^+$ T cells, including intracellular delays. The authors argue that a good strategy to control HIV should focus on drugs to prolong the latent period and/or slow down the virus production.

In this paper, we propose a model for the three stages of HIV infection, including drug-resistance. We study the integer-order model and its fractional order counterpart. In Section 2, we describe the model, and, in Section 3, compute the reproduction number and the local stability of the disease-free equilibrium. In Section 4, we analyze several simulations of the integer-order and fractional-order versions of the model, and discuss implications of the results. Finally, we conclude our work in Section 5, and point out some future research.

1.1 Some concepts of fractional calculus

Fractional calculus (FC) is a generalization to an arbitrary (non-integer) order of ordinary differentiation and integration. Leibniz and Newton were the first mathematicians to discover and unravel the power of FC. Leibniz wrote a letter to L'Hôpital, in 1695, where he questioned the possibility of generalizing the concept of integer order derivatives to non-integer orders. L'Hôpital asked what would be the consequences of considering a $1/2$ order derivative. Leibniz ends the letter exchange stating that $1/2$ order would be a paradox leading to useful consequences in the future. More on fractional calculus can be seen in [8,9,10,11,12,13].

FC has been applied, in the last few decades, to a large variety of scientific problems. Some important applications are in engineering [14,15,16,17], physics [18], biology [19,20], and others.

The concept of fractional-order derivative has been formulated in different, but equivalent, ways. The most usual definitions are the Riemann-Liouville, the Grünwald-Letnikov (GL), and the Caputo formulations [10,8]. Here, we use the GL derivative, given by equation (1).

$$ {}_a^{\mathrm{GL}}D_t^{\alpha} f(t) = \lim_{h\to 0} \frac{1}{h^{\alpha}} \sum_{k=0}^{\left[\frac{t-a}{h}\right]} (-1)^k \binom{\alpha}{k} f(t-kh), \; t > a, \; \alpha > 0 \tag{1} $$

where $[x]$ means the integer part of x, and h represents the time step increment.

The GL definition inspired a discrete-time calculation algorithm, based on the approximation of the time increment h by means of the sampling perid T. A practical implementation is achieved with the r-term truncated series given by:

$$ \frac{\mathscr{Z}\{D^{\alpha} f(t)\}}{\mathscr{Z}\{f(t)\}} = \frac{1}{T^{\alpha}} \sum_{k=0}^{r} \frac{(-1)^k \Gamma(\alpha+1)}{k!\,\Gamma(\alpha-k+1)} z^{-k} \tag{2} $$

where, in order to have good approximations, it is required a large r and a small value of T.

Expression (2) represents the Euler, or first backward difference, approximation in the so-called $s \to z$ conversion scheme. Another possibility, consists in the Tustin conversion rule. The most often adopted generalization of the generalized derivative operator consists in $\alpha \in \mathbf{R}$.

2 Description of the model

The model describes the dynamics of the T cells populations, macrophages, CTLs and viruses. There are nine compartments, namely, the uninfected CD4$^+$ T cells, T, susceptible T cells, T_s, resistant T cells, T_r, macrophages, M, susceptible macrophage, M_s, resistant macrophages, M_r, CTLs, Z, susceptible viruses, V_s, and resistant viruses, V_r.

The first two terms in the equations modeling the T and M cells, represent the source of new T and M cells, respectively. CTLs are generated by the first three terms of the corresponding equation. The logistic term of the T cells prevents its number to exceed the maximum concentration T_{max}. The infection parameters k_1, k_2, k_4 denote cells' infection by viruses and infected macrophages. Rates k_3, k_5 denote the killing of the infected helper cells and macrophages by CTLs, respectively. Death rates are represented by δ_i. Viruses are cleared at a rate c. The dynamics concerning drug-resistance is as follows. Parameters t_1, $t_2 \in [0,1]$, represent the efficacy of RTIs and PIs, respectively. A value of 0 is associated with non-treatment and a value of 1 with full treatment. RTIs inhibit the infection of CD4$^+$ T cells and macrophages by viruses. On the other hand, PIs prevent the production of infectious viruses from already infected cells.

Drug resistance results in the inability of RTIs to inhibit the infection of cells by resistant viruses. As a result, infection rates by mutated viruses are considered to be reduced. The same applies to the protease enzyme, thereby reducing the

virus' replicative capacity. All these factors suggest that mutated virus is less fit than the wild-type in terms of infecting and replicating capacity. This fitness factor is incorporated in the model equations above through parameter ψ. The efficacy of the drugs on macrophages is $f_i t_i$, where $f_i \in [0,1]$ and subindex i refers to each drug. Drug efficacy in macrophages is lower than in CD4$^+$ T cells. Any viral mutations are accounted in the model via the parameter u, which represents the probability of mutation per replication cycle. V_s and V_r particles are produced by the corresponding infected CD4$^+$ and macrophages populations, with bursting sizes of drug-sensitive strain, N_s, and of drug-resistant strain, N_r.

The schematic diagram of the model can be found in Figure 1.

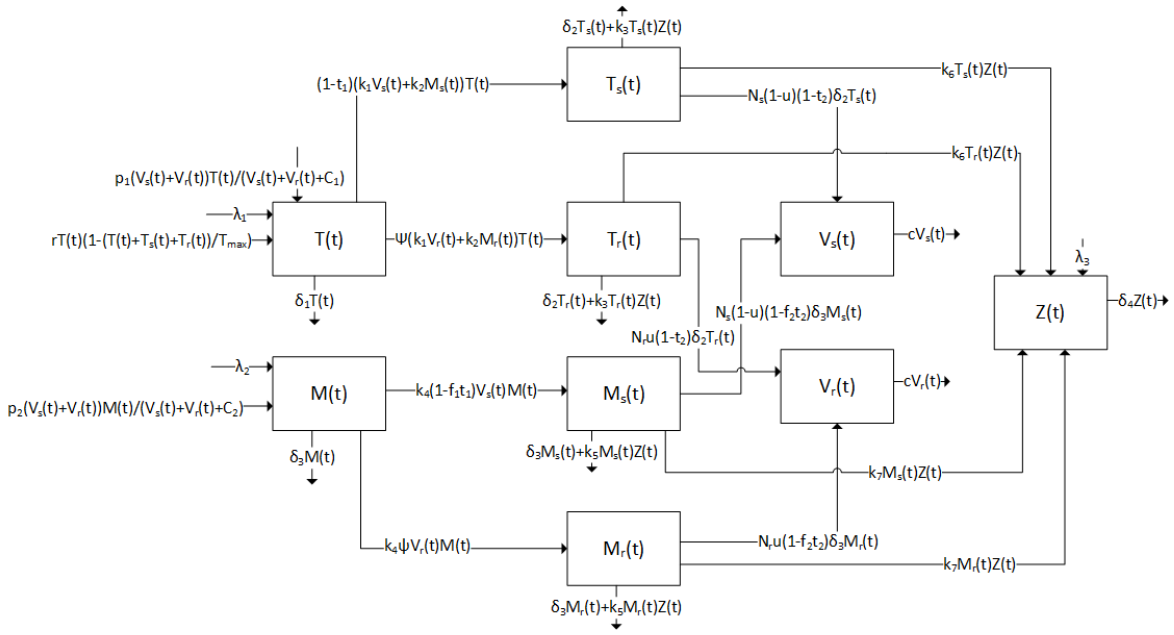

Fig. 1: Schematic diagram of the model (3).

The nonlinear fractional order system describing the dynamics of the model is:

$$
\begin{aligned}
\frac{dT^{\alpha}(t)}{dt^{\alpha}} &= \lambda_1 + \frac{p_1(V_s(t)+V_r(t))}{V_s(t)+V_r(t)+C_1}T(t) + rT(t)(1-(T(t)+T_s(t)+T_r(t))/T_{max}) + \\
&\quad -(1-t_1)(k_1V_s(t)+k_2M_s(t))T(t) - \psi(k_1V_r(t)+k_2M_r(t))T(t) - \delta_1 T(t) \\
\frac{dT_s^{\alpha}(t)}{dt^{\alpha}} &= (1-t_1)(k_1V_s(t)+k_2M_s(t))T(t) - k_3T_s(t)Z(t) - \delta_2 T_s(t) \\
\frac{dT_r^{\alpha}(t)}{dt^{\alpha}} &= \psi(k_1V_r(t)+k_2M_r(t))T(t) - k_3T_r(t)Z(t) - \delta_2 T_r(t) \\
\frac{dM^{\alpha}(t)}{dt^{\alpha}} &= \lambda_2 + \frac{p_2(V_s(t)+V_r(t))}{C_2+V_s(t)+V_r(t)}M(t) - k_4(1-f_1t_1)V_s(t)M(t) - k_4\psi V_r(t)M(t) - \delta_3 M(t) \\
\frac{dM_s^{\alpha}(t)}{dt^{\alpha}} &= k_4(1-f_1t_1)V_s(t)M(t) - k_5M_s(t)Z(t) - \delta_3 M_s(t) \\
\frac{dM_r^{\alpha}(t)}{dt^{\alpha}} &= k_4\psi V_r(t)M(t) - k_5M_r(t)Z(t) - \delta_3 M_r(t) \\
\frac{dV_s^{\alpha}(t)}{dt^{\alpha}} &= N_s(1-u)((1-t_2)\delta_2 T_s + (1-f_2t_2)\delta_3 M_s) - cV_s(t) \\
\frac{dV_r^{\alpha}(t)}{dt^{\alpha}} &= N_r u((1-t_2)\delta_2 T_r + (1-f_2t_2)\delta_3 M_r) - cV_r(r) \\
\frac{dZ^{\alpha}(t)}{dt^{\alpha}} &= \lambda_3 + k_6(T_s(t)+T_r(t))Z(t) + k_7(M_s(t)+M_r(t))Z(t) - \delta_4 Z(t)
\end{aligned}
\tag{3}
$$

3 Stability of equilibria

In this subsection, we compute the stability of equilibria of the fractional model (3).

We begin by considering two sub-models of model (3). Model (4) is obtained from model (3) by setting the variables concerning resistance dynamics (T_r, M_r and V_r) to zero. On the other hand, model (7) follows from model (3) by setting the variables concerning sensitive dynamics (T_s, M_s and V_s) to zero.

$$\begin{aligned}
\frac{dT^{\alpha}(t)}{dt^{\alpha}} &= \lambda_1 + \frac{p_1 V_s(t)}{V_s(t)+C_1} T(t) + rT(t)(1-(T(t)+T_s(t))/T_{max}) \\
&\quad -(1-t_1)(k_1 V_s(t)+k_2 M_s(t))T(t) - \delta_1 T(t) \\
\frac{dT_s^{\alpha}(t)}{dt^{\alpha}} &= (1-t_1)(k_1 V_s(t)+k_2 M_s(t))T(t) - k_3 T_s(t) Z(t) - \delta_2 T_s(t) \\
\frac{dM^{\alpha}(t)}{dt^{\alpha}} &= \lambda_2 + \frac{p_2 V_s(t)}{C_2+V_s(t)} M(t) - k_4(1-f_1 t_1) V_s(t) M(t) - \delta_3 M(t) \\
\frac{dM_s^{\alpha}(t)}{dt^{\alpha}} &= k_4(1-f_1 t_1) V_s(t) M(t) - k_5 M_s(t) Z(t) - \delta_3 M_s(t) \\
\frac{dV_s^{\alpha}(t)}{dt^{\alpha}} &= N_s(1-u)((1-t_2)\delta_2 T_s + (1-f_2 t_2)\delta_3 M_s) - cV_s(t) \\
\frac{dZ^{\alpha}(t)}{dt^{\alpha}} &= \lambda_3 + k_6 T_s(t) Z(t) + k_7 M_s(t) Z(t) - \delta_4 Z(t)
\end{aligned} \tag{4}$$

The disease-free equilibrium of model (4) is given by:

$$\begin{aligned}
P_0^1 &= (T^0, T_s^0, M^0, M_s^0, V_s^0, Z^0) = \\
&= \left(\frac{T_{max}\left[(r-\delta_1)+\sqrt{(r-\delta_1)^2+\frac{4r\lambda_1}{T_{max}}}\right]}{2r}, 0, \frac{\lambda_2}{\delta_3}, 0, 0, \frac{\lambda_3}{\delta_4} \right)
\end{aligned} \tag{5}$$

Lemma 1. *The disease-free equilibrium P_0^1 is locally asymptotically stable if all eigenvalues λ_i of the linearization matrix of model (4), satisfy $|\arg(\lambda_i)| > \alpha\frac{\pi}{2}$.*

Proof. The linearization matrix of model (4) at the disease-free equilibrium P_0^1 is as follows:

$$M_1 = \begin{pmatrix}
r\left(1-\frac{2T^0}{T_{max}}\right)-\delta_1 & -\frac{rT^0}{T_{max}} & 0 & -(1-t_1)k_2T^0 & \frac{p_1T^0}{C_1}-(1-t_1)k_1T^0 & 0 \\
0 & -\delta_2-k_3Z^0 & 0 & (1-t_1)k_2T^0 & (1-t_1)k_1T^0 & 0 \\
0 & 0 & -\delta_3 & 0 & \frac{p_2M^0}{C_2}-k_4(1-f_1t_1)M^0 & 0 \\
0 & 0 & 0 & -\delta_3-k_5Z^0 & k_4(1-f_1t_1)M^0 & 0 \\
0 & N_s(1-u)(1-t_2)\delta_2 & 0 & N_s(1-u)(1-f_2t_2)\delta_3 & -c & 0 \\
0 & k_6Z^0 & 0 & k_7Z^0 & 0 & -\delta_4
\end{pmatrix}$$

The following eigenvalues are easily obtained and are all real and negative:

$$r\left(1-\frac{2T^0}{T_{max}}\right)-\delta_1, \qquad -\delta_3, \qquad -\delta_4,$$

The remaining eigenvalues are the roots of the characteristic equation of the 3×3 matrix, M_2, given below:

$$M_2 = \begin{pmatrix}
-\delta_2-k_3Z^0 & (1-t_1)k_2T^0 & (1-t_1)k_1T^0 \\
0 & -\delta_3-k_5Z^0 & k_4(1-f_1t_1)M^0 \\
N_s(1-u)(1-t_2)\delta_2 & N_s(1-u)(1-f_2t_2)\delta_3 & -c
\end{pmatrix} = \begin{pmatrix}
-A & (1-t_1)k_2T^0 & (1-t_1)k_1T^0 \\
0 & -B & k_4(1-f_1t_1)M^0 \\
N_s(1-u)D & N_s(1-u)E & -c
\end{pmatrix}$$

The determinant $|M_2-\lambda I_3|=0$, where I_3 is the identity matrix of order 3, is equivalent to:

$$\begin{aligned}
&(-A-\lambda)(-B-\lambda)(-c-\lambda)+(1-t_1)k_2T^0k_4(1-f_1t_1)M^0N_s(1-u)D+ \\
&-N_s(1-u)D(-B-\lambda)(1-t_1)k_1T^0-N_s(1-u)Ek_4(1-f_1t_1)M^0(-A-\lambda)=0 \Leftrightarrow \\
&(-A-\lambda)(-B-\lambda)(-c-\lambda)+(1-t_1)k_2T^0HcD-GcD(-B-\lambda)-HcE(-A-\lambda)=0 \Leftrightarrow \\
&\lambda^3+(A+B+c)\lambda^2+(AB+Ac+Bc-GcD-HcE)\lambda+ABc-(1-t_1)k_2T^0HcD-BGcD-HcEA=0
\end{aligned}$$

Thus, the characteristic polynomial is:

$$P_1(\lambda) = \lambda^3 + a_1\lambda^2 + a_2\lambda + a_3 \tag{6}$$

where $a_1 = A+B+c$, $a_2 = AB+Ac+Bc-GDc-HEc$, $a_3 = ABc-(1-t_1)k_2T^0HDc-BGDc-HEAc$, $G=\frac{(1-t_1)k_1T^0N_s(1-u)}{c}$, and $H=\frac{(1-f_1t_1)k_4M^0N_s(1-u)}{c}$.

Let $D(P)$ be the discriminant of the characteristic polynomial P of matrix M_2. Thus:

$$D(P) = -\begin{vmatrix} 1 & a_1 & a_2 & a_3 & 0 \\ 0 & 1 & a_1 & a_2 & a_3 \\ 3 & 2a_1 & a_2 & 0 & 0 \\ 0 & 3 & 2a_1 & a_2 & 0 \\ 0 & 0 & 3 & 2a_1 & a_2 \end{vmatrix} = 18a_1a_2a_3 + (a_1a_2)^2 - 4a_3a_1^3 - 4a_2^3 - 27a_3^2$$

Ahmed *et al* [21] study some Routh-Hurwitz stability conditions for fractional order systems. If $D(P) > 0$ the well known Routh-Hurwitz conditions are necessary and sufficient for $|\arg(\lambda_i)| > \alpha\frac{\pi}{2}$ to be true, i.e.:

$$a_1 > 0,\ a_3 > 0,\ a_1a_2 > a_3$$

These conditions and the discriminant $D(P)$ are computed and are shown to be greater than zero for the parameter values given in Table 1. We obtain:

$$\begin{aligned} a_1 = 23.01 > 0; \quad a_2 = 0.1771 > 0; \quad a_3 = 0.0003 > 0 \\ a_1a_2 = 4.0756 > a_3;\ D(P) = 1.5673 > 0 \end{aligned}$$

Thus, the disease-free equilibrium P_0^1 is locally asymptotically stable for $\alpha \in [0,1)$.

We proceed with the study of the stability of the disease-free equilibrium, P_0^2, of model (7).

$$\begin{aligned} \dot{T}(t) &= \lambda_1 + \tfrac{p_1V_r(t)}{V_r(t)+C_1}T(t) + rT(t)(1-(T(t)+T_r(t))/T_{max}) \\ &\quad -\psi(k_1V_r(t)+k_2M_r(t))T(t) - \delta_1T(t) \\ \dot{T}_r(t) &= \psi(k_1V_r(t)+k_2M_r(t))T(t) - \delta_2T_r(t) - k_3T_r(t)Z(t) \\ \dot{M}(t) &= \lambda_2 + \tfrac{p_2V_r(t)}{C_2+V_r(t)}M(t) - k_4\psi V_r(t)M(t) - \delta_3M(t) \\ \dot{M}_r(t) &= k_4\psi V_r(t)M(t) - k_5M_r(t)Z(t) - \delta_3M_r(t) \\ \dot{V}_r(t) &= N_ru((1-t_2)\delta_2T_r + (1-f_2t_2)\delta_3M_r) - cV_r(r) \\ \dot{Z}(t) &= \lambda_3 + k_6T_r(t)Z(t) + k_7M_r(t)Z(t) - \delta_4Z(t) \end{aligned} \tag{7}$$

The disease-free equilibrium state P_0^2 of model (7) is given by:

$$\begin{aligned} P_0^2 &= (T^0, T_r^0, M^0, M_r^0, V_r^0, Z^0) \\ &= \left(\frac{T_{max}\left[(r-\delta_1)+\sqrt{(r-\delta_1)^2+\frac{4r\lambda_1}{T_{max}}}\right]}{2r}, 0, \frac{\lambda_2}{\delta_3}, 0, 0, \frac{\lambda_3}{\delta_4} \right) \end{aligned} \tag{8}$$

Lemma 2.*The disease-free equilibrium P_0^2 is locally asymptotically stable if all eigenvalues λ_i of the linearization matrix of model (7), satisfy $|\arg(\lambda_i)| > \alpha\frac{\pi}{2}$.*

*Proof.*The linearization matrix of the model (7) at P_0^2 is given by:

$$M_3 = \begin{pmatrix} r\left(1-\frac{2T^0}{T_{max}}\right)-\delta_1 & -\frac{rT^0}{T_{max}} & 0 & -\psi k_2T^0 & \frac{p_1T^0}{C_1} - \psi k_1T^0 & 0 \\ 0 & -\delta_2 - k_3Z^0 & 0 & \psi k_2T^0 & \psi k_1T^0 & 0 \\ 0 & 0 & -\delta_3 & 0 & \frac{p_2M^0}{C_2} - k_4\psi M^0 & 0 \\ 0 & 0 & 0 & -\delta_3 - k_5Z^0 & k_4\psi M^0 & 0 \\ 0 & N_ru(1-t_2)\delta_2 & 0 & N_ru(1-f_2t_2)\delta_3 & -c & 0 \\ 0 & k_6Z^0 & 0 & k_7Z^0 & 0 & -\delta_4 \end{pmatrix}$$

The following eigenvalues are easily obtained and are all real and negative:

$$r\left(1-\frac{2T^0}{T_{max}}\right)-\delta_1, \qquad -\delta_3, \qquad -\delta_4,$$

The remaining eigenvalues are the roots of the characteristic equation of a 3×3 matrix, M_4, given by:

$$M_4 = \begin{pmatrix} -\delta_2 - k_3 Z^0 & \psi k_2 T^0 & \psi k_1 T^0 \\ 0 & -\delta_3 - k_5 Z^0 & k_4 \psi M^0 \\ N_r u(1-t_2)\delta_2 & N_r u(1-f_2 t_2)\delta_3 & -c \end{pmatrix} = \begin{pmatrix} -A & \psi k_2 T^0 & \psi k_1 T^0 \\ 0 & -B & k_4 \psi M^0 \\ N_r uD & N_r uE & -c \end{pmatrix}$$

The determinant $|M_4 - \lambda I_3| = 0$ is equivalent to:

$$(-A-\lambda)(-B-\lambda)(-c-\lambda) + \psi k_2 T^0 k_4 \psi M^0 N_r uD - N_r uD(-B-\lambda)\psi k_1 T^0 - N_r uE k_4 \psi M^0 (-A-\lambda) = 0$$
$$(-A-\lambda)(-B-\lambda)(-c-\lambda) + \psi k_2 T^0 JcD - IcD(-B-\lambda) - JcE(-A-\lambda) = 0$$

where $I = \frac{\psi k_1 N_r u T^0}{c}$, $J = \frac{\psi k_4 N_r u M^0}{c}$. The characteristic polynomial associated to matrix M_4 is thus:

$$P_2(\lambda) = \lambda^3 + a_1\lambda^2 + a_2\lambda + a_3 \tag{9}$$

where $a_1 = A+B+c$, $a_2 = AB+Ac+Bc-IDc-JEc$, and $a_3 = ABc - \psi k_2 T^0 JDc - IDBc - JEAc$. Let $D(P) = 18a_1a_2a_3 + (a_1a_2)^2 - 4a_3a_1^3 - 4a_2^3 - 27a_3^2$ be the discriminant of the characteristic polynomial $P_2(\lambda)$ of matrix M_4. Following Ahmed *et al* [21], if $D(P) > 0$ the Routh-Hurwitz conditions are necessary and sufficient for $|\arg(\lambda_i)| > \alpha\frac{\pi}{2}$ to be true, i.e.:

$$a_1 > 0,\ a_3 > 0,\ a_1a_2 > a_3$$

These conditions and the discriminant $D(P)$ are computed and are shown to be greater than zero for the parameter values given in Table 1. We obtain:

$$a_1 = 23.01 > 0; \quad a_2 = 0.2308 > 0; \quad a_3 = 0.0005 > 0$$
$$a_1a_2 = 5.31 > a_3;\ D(P) = 0.0002 > 0$$

Thus, the disease-free equilibrium P_0^2 is locally asymptotically stable for $\alpha \in [0,1)$.

We continue with the study of the stability of the disease-free equilibrium of the full model (3). The disease-free equilibrium state, P_0, of model (3) is given by:

$$\begin{aligned} P_0 &= (T^0, T_s^0, T_r^0, M^0, M_s^0, M_r^0, V_s^0, V_r^0, Z^0) \\ &= \left(\frac{T_{max}\left[(r-\delta_1) + \sqrt{(r-\delta_1)^2 + \frac{4r\lambda_1}{T_{max}}}\right]}{2r}, 0, 0, \frac{\lambda_2}{\delta_3}, 0, 0, 0, 0, \frac{\lambda_3}{\delta_4} \right) \end{aligned} \tag{10}$$

Lemma 3. *The disease-free equilibrium P_0 is locally asymptotically stable if all eigenvalues λ_i of the linearization matrix of model (3), satisfy $|\arg(\lambda_i)| > \alpha\frac{\pi}{2}$.*

Proof. The linearization matrix of model (3) around the disease-free equilibrium P_0 is given by:

$$M_5 = \begin{pmatrix} r\left(1-\frac{2T^0}{T_{max}}\right) - \delta_1 & -\frac{rT^0}{T_{max}} & -\frac{rT^0}{T_{max}} & 0 & -(1-t_1)k_2T^0 & -\psi k_2 T^0 & \frac{p_1}{C_1}T^0 - (1-t_1)k_1T^0 & \frac{p_1}{C_1}T^0 - \psi k_1 T^0 & 0 \\ 0 & -\delta_2 - k_3 Z^0 & 0 & 0 & (1-t_1)k_2T^0 & 0 & (1-t_1)k_1T^0 & 0 & 0 \\ 0 & 0 & -\delta_2 - k_3 Z^0 & 0 & 0 & \psi k_2 T^0 & 0 & \psi k_1 T^0 & 0 \\ 0 & 0 & 0 & -\delta_3 & 0 & 0 & \frac{p_2}{C_2}M^0 - k_4(1-f_1t_1)M^0 & \frac{p_2}{C_2}M^0 - k_4\psi M^0 & 0 \\ 0 & 0 & 0 & 0 & -\delta_3 - k_5 Z^0 & 0 & k_4(1-f_1t_1)M^0 & 0 & 0 \\ 0 & 0 & 0 & 0 & 0 & -\delta_3 - k_5 Z^0 & 0 & k_4\psi M^0 & 0 \\ 0 & N_s(1-u)(1-t_2)\delta_2 & 0 & 0 & N_s(1-u)(1-f_2t_2)\delta_3 & 0 & -c & 0 & 0 \\ 0 & 0 & N_r u(1-t_2)\delta_2 & 0 & 0 & N_r u(1-f_2t_2)\delta_3 & 0 & -c & 0 \\ 0 & k_6 Z^0 & k_6 Z^0 & 0 & k_7 Z^0 & k_7 Z^0 & 0 & 0 & -\delta_4 \end{pmatrix}$$

The following eigenvalues are all real and negative, and easily obtained:

$$r\left(1-\frac{2T^0}{T_{max}}\right) - \delta_1, \qquad -\delta_3, \qquad -\delta_4,$$

The remaining eigenvalues are the roots of the characteristic equation of a 6×6 matrix, M_6, given by:

$$M_6 = \begin{pmatrix} -\delta_2 - k_3 Z^0 & 0 & (1-t_1)k_2 T^0 & 0 & (1-t_1)k_1 T^0 & 0 \\ 0 & -\delta_2 - k_3 Z^0 & 0 & \psi k_2 T^0 & 0 & \psi k_1 T^0 \\ 0 & 0 & -\delta_3 - k_5 Z^0 & 0 & k_4(1-f_1 t_1)M^0 & 0 \\ 0 & 0 & 0 & -\delta_3 - k_5 Z^0 & 0 & k_4 \psi M^0 \\ N_s(1-u)(1-t_2)\delta_2 & 0 & N_s(1-u)(1-f_2 t_2)\delta_3 & 0 & -c & 0 \\ 0 & N_r u(1-t_2)\delta_2 & 0 & N_r u(1-f_2 t_2)\delta_3 & 0 & -c \end{pmatrix}$$

$$= \begin{pmatrix} -A & 0 & (1-t_1)k_2 T^0 & 0 & (1-t_1)k_1 T^0 & 0 \\ 0 & -A & 0 & \psi k_2 T^0 & 0 & \psi k_1 T^0 \\ 0 & 0 & -B & 0 & k_4(1-f_1 t_1)M^0 & 0 \\ 0 & 0 & 0 & -B & 0 & k_4 \psi M^0 \\ N_s(1-u)D & 0 & N_s(1-u)E & 0 & -c & 0 \\ 0 & N_r u D & 0 & N_r u E & 0 & -c \end{pmatrix}$$

The determinant $|M_6 - \lambda I_6| = 0$, where I_6 is the identity matrix of order 6, is equivalent to:

$$\begin{aligned} &(-A-\lambda)^2(-B-\lambda)\left[(-B-\lambda)(-c-\lambda)^2 - N_r u E(-c-\lambda)k_4\psi M^0\right] + (-A-\lambda)^2 N_s(1-u)E\left[k_4(1-f_1t_1)M^0 k_4 \psi M^0 N_r u E - \right. \\ &\left.(-c-\lambda)(-B-\lambda)k_4(1-f_1t_1)M^0\right] - (-A-\lambda)N_r u D(-B-\lambda)\left[\psi k_1 T^0(-B-\lambda)(-c-\lambda) - \right. \\ &\left.(-c-\lambda)k_4\psi M^0 \psi k_2 T^0\right] - (-A-\lambda)N_r u D N_s(1-u)E\left[\psi k_2 T^0 k_4(1-f_1t_1)M^0 k_4 \psi M^0 - \right. \\ &\left.(-B-\lambda)k_4(1-f_1t_1)M^0 \psi k_1 T^0\right] - N_s(1-u)D(-A-\lambda)(1-t_1)k_2 T^0\left[k_4(1-f_1t_1)M^0 k_4 \psi M^0 N_r u E \right. \\ &\left.-(-c-\lambda)(-B-\lambda)k_4(1-f_1t_1)M^0\right] + N_s(1-u)D(-A-\lambda)(-B-\lambda)\times \\ &\left[(1-t_1)k_1 T^0 k_4 \psi M^0 N_r u E - (-c-\lambda)(-B-\lambda)(1-t_1)k_1 T^0\right] + \\ &+N_s(1-u)D N_r u D(1-t_1)k_2 T^0\left[\psi k_2 T^0 k_4(1-f_1t_1)M^0 k_4 \psi M^0 - (-B-\lambda)k_4(1-f_1t_1)M^0 \psi k_1 T^0\right] + \\ &+N_s(1-u)D N_r u D(-B-\lambda)\left[(1-t_1)k_1 T^0 \psi k_1 T^0(-B-\lambda) - k_4 \psi M^0 \psi k_2 T^0(1-t_1)k_1 T^0\right] = 0 \end{aligned}$$

After some algebra manipulation, we obtain:

$$\begin{aligned} &\left[(-A-\lambda)(-B-\lambda)(-c-\lambda) - (-A-\lambda)N_s(1-u)E k_4(1-f_1t_1)M^0 + \right. \\ &\left.+N_s(1-u)D(1-t_1)k_2 T^0 k_4(1-f_1t_1)M^0 - N_s(1-u)D(-B-\lambda)(1-t_1)k_1 T^0\right] = 0 \end{aligned}$$

$$P(\lambda) = \left[(-A-\lambda)(-B-\lambda)(-c-\lambda) - (-A-\lambda)N_r u E k_4 \psi M^0 + N_r u D k_4 \psi M^0 \psi k_2 T^0 - N_r u D \psi k_1 T^0(-B-\lambda)\right] = 0$$

The first term of the characteristic polynomial $P(\lambda)$ is the characteristic polynomial of matrix M_2 (6) and the second term is the characteristic polynomial of matrix M_4 (9). Thus, as it is shown above, the disease-free equilibria P_0^1 and P_0^2 are locally asymptotically stable, then P_0 is also locally asymptotically stable for $\alpha \in [0,1)$.

4 Numerical Results

In this section we present the numerical results for models (3). The parameters used in the simulations are given in Table 1 and the initial conditions are set to $T(0) = 1000$, $M(0) = 30$, $Z(0) = 333$, and all other variables are set to 0.001.

Figure 2 depicts the dynamics of the disease-free equilibrium (DF) for $\alpha \in \{0.5, 0.6, 0.7, 0.8, 0.9, 1.0\}$.

In Figures 3-4, we observe the dynamics of the rapid progressors (RP) and of the long-term non progressors (LTNP) of the model (3), respectively, for $\alpha \in \{0.5, 0.6, 0.7, 0.8, 0.9, 1.0\}$. RP are untreated patients whose $CD4^+$ T cells decrease below the AIDS threshold after, approximately, 3-5 years [24]. On the other hand, LTNP are HIV patients, who without therapy, manage to escape the common route to AIDS for 15-20 years. RP and LTNP account for 10% and $10-17$%, respectively, of HIV infected patients [25]. Most non-treated patients, living with HIV, progress to AIDS within 8-10 years, after initial infection. Differences in the progression route to AIDS have been associated with patients' immune system status, genetic profile, and age [24].

From the observation of Figs. 2-4, some interesting features arise. Faster transients and slower evolutions towards the disease-free equilibrium, RP and LTNP states, as α is decreased from 1. Moreover, these distinct patterns for decreasing α may bring new insights in the understanding of distinct progression routes to AIDS in individuals. We mean by this that the fractional model (3) may help to predict when a particular individual will change its HIV progression status, thus helping the clinician to advise, in advance, the initiation or the change of HAART regimen. The diversity of patterns, observed in the fractional model, are somewhat masked by the mean behavior seen in the deterministic models. There are current studies that suggest the use of the cumulative individual HIV viremia, defined as the area under the curve of the log viral load of each individual, to predict AIDS-related and non-AIDS-related malignancies [26]. Early treatment and therapy adherence are considered crucial to reduce cumulative individual HIV burden. Thus, better predictions of the viral load curve, induce better clinical judgment, improving patients' well being.

We expect to validate this claim in a near future, using data from Portuguese HIV infected patients.

Parameter	DF	RP	LTNP	Reference
λ_1	10	10	35	[5]
λ_2	0.15	0.15	0.15	[5]
λ_3	5	5	4	[5]
δ_1	0.02	0.02	0.01	[5]
δ_2	0.28	0.28	0.28	[5]
δ_3	0.005	0.0045	0.005	[5]
δ_4	0.015	0.015	0.028	[5]
r	0.03	0.072	0.072	[5]
c	23	8	10	
T_{max}	1500	1500	1500	[22]
C_1	300	300	300	[6]
C_2	220	220	200	[6]
t_1	0	0	0	[5]
t_2	0	0	0	[5]
u	0.01	0.001	0.001	[5]
ψ	0.9	0.9	0.9	[5]
p_1	0.048	0.048	0.065	[5]
p_2	0.0078	0.0078	0.0068	[5]
k_1	4.0×10^{-8}	4.0×10^{-5}	2.5×10^{-5}	[23]
k_2	1×10^{-8}	1×10^{-8}	9.8×10^{-9}	[23]
k_3	9.9×10^{-8}	9.9×10^{-8}	9.9×10^{-4}	[23]
k_4	4.22×10^{-8}	4.22×10^{-8}	4.22×10^{-8}	[23]
k_5	6.6×10^{-6}	6.6×10^{-6}	9.6×10^{-6}	[23]
k_6	2.63×10^{-4}	2.3×10^{-4}	3.93×10^{-4}	[23]
k_7	5.28×10^{-9}	5.28×10^{-9}	6.6×10^{-9}	[23]
N_s	4800	4800	3000	[22]
N_r	3000	3000	2000	[22]
f_1	0.34	0.34	0.34	[5]
f_2	0.34	0.34	0.34	[5]

Table 1: Parameters used in the numerical simulations of model (3). DF - disease-free equilibrium; RP - rapid progressor; LTNP - long-term non progressor.

5 Conclusion

We analyze a fractional order model for the three-stages of HIV infection, including drug-resistance. We compute the stability of the disease-free equilibrium. The fractional model depicts a broad variety of dynamics for the disease-free, RP and the LTNP states. The later may help to explain peculiarities between individuals' progression to AIDS, that may help clinicians to advise, 'a priori' changes or initiation of HAART regimen, contributing to patients' well being. This conclusion will be validated with real data in a near future.

Acknowledgements

Authors wish to thank the Polytechnic of Porto, through the PAPRE Programa de Apoio à Publicação em Revistas Científicas de Elevada Qualidade for financial support. The authors were partially funded by the European Regional Development Fund through the program COMPETE and by the Portuguese Government through the FCT - Fundação para a Ciência e a Tecnologia under the project PEst-C/MAT/UI0144/2013. The research of AC was partially supported by a FCT grant with reference SFRH/BD/96816/2013.

References

[1] M. Pitchaimani, C. Monica and M. Divya, Stability analysis for HIV infection delay model with protease inhibitor, *BioSystems* **114**, 118–124 (2013).
[2] X. Wei, S.K. Ghosh, M.E. Taylor, V. A. Johnson, E.A. Emini, P. Deutsch, J.D. Lifson, S. Bonhoeffer, M.A. Nowak, B.H. Hahn et al., Viral dynamics in human immune deficiency virus type 1 infection, *Nature* **373**, 117–122 (1995).
[3] L.M. Wahl and M.A. Nowak, Adherence and drug resistance: predictions for therapy outcome, *Proc. Royal Soc. Biol. Sci.* **267**, 835–843 (2000).
[4] A.S. Perelson, A.U. Neumann, M. Markowitz, J.M. Leonard and D.D. Ho, HIV-1 dynamics in vivo: virion clearance rate, infected cell life-span, and viral generation time, *Science* **271**, 1582–1586 (1996).

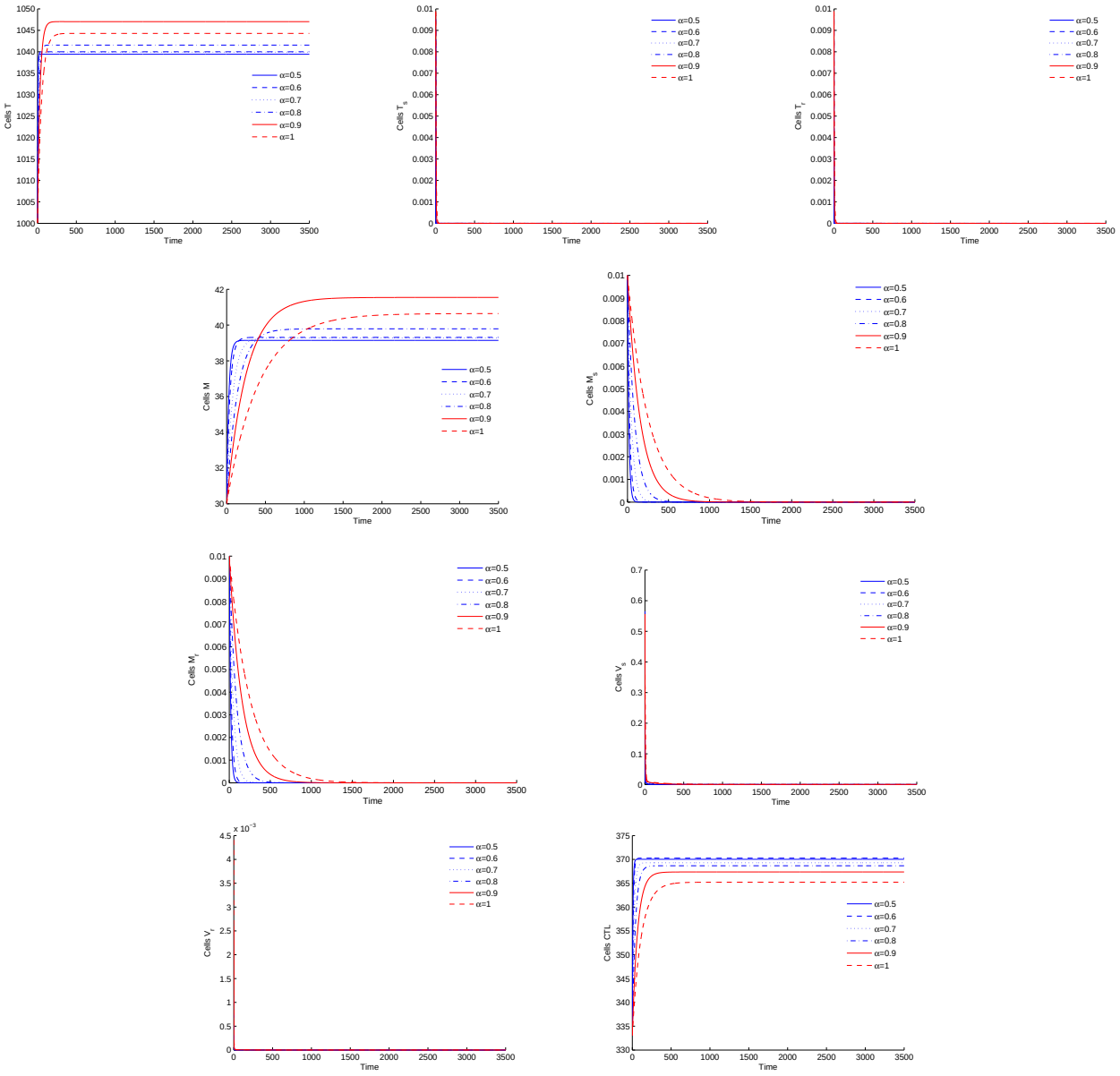

Fig. 2: Dynamics of disease-free equilibrium of the fractional order model (3) for $\alpha \in \{0.5, 0.6, 0.7, 0.8, 0.9, 1.0\}$. Parameter values are those of Table 1 and initial conditions are given in the text.

[5] M.M. Hadjiandreou, R. Conejeros and D.I. Wilson, Long-term HIV dynamics subject to continuous therapy and structured treatment interruptions, *Chem. Eng. Sci.* **64**, 1600–1617 (2009).

[6] E. A. Hernandez-Vargas and R.H. Middleton, Modeling the three stages of HIV infection, *J. Theor. Biol.*, **320**, 33–40 (2013).

[7] C.M.A. Pinto and A.R.M. Carvalho, Mathematical model for HIV dynamics in HIV-specific helper cells, *Commun. Nonlin. Sci.* **19**, 693–701 (2014).

[8] K.B. Oldham and J. Spanier, *The fractional calculus: theory and application of differentiation and integration to arbitrary order*, Academic Press, 1974.

[9] S.G. Samko, A.A. Kilbas and O.I. Marichev, *Fractional integrals and derivatives: theory and applications*, Gordon and Breach Science Publishers, 1993.

[10] K.S. Miller and B. Ross, *An introduction to the fractional calculus and fractional differential equations*, John Wiley and Sons, 1993.

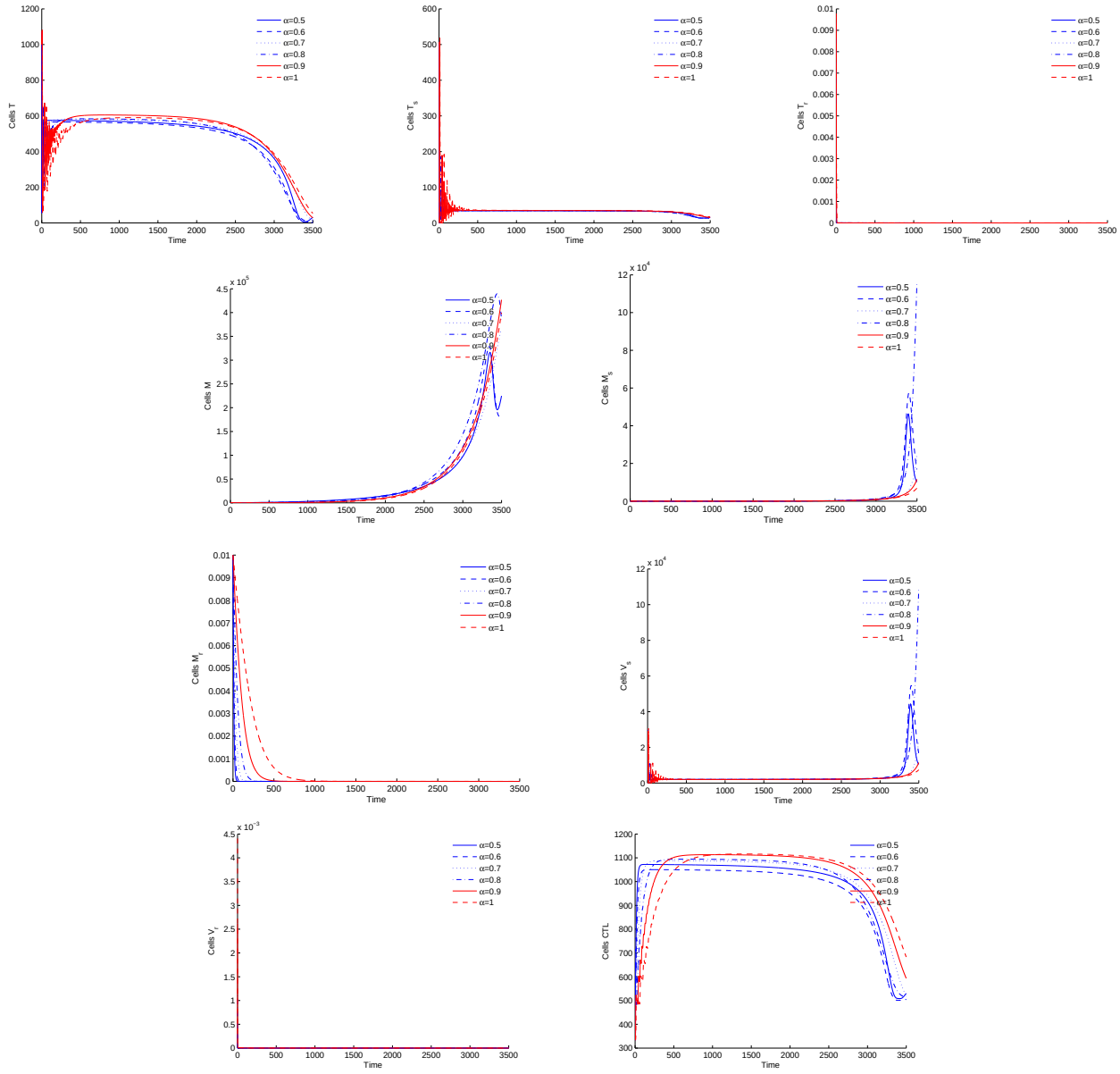

Fig. 3: Dynamics of the rapid progressors of the fractional order model (3) for $\alpha \in \{0.5, 0.6, 0.7, 0.8, 0.9, 1.0\}$. Parameter values are those of Table 1 and initial conditions are given in the text.

[11] V.E. Tarasov, *Fractional dynamics: Applications of fractional calculus to dynamics of particles, fields and media*, Springer, New York, 2010.
[12] D. Baleanu, K. Diethelm, E. Scalas and J. J. Trujillo, *Fractional Calculus Models and Numerical Methods* (Series on Complexity, Nonlinearity and Chaos), World Scientific, Singapore, 2012.
[13] A. Atangana and E. Alabaraoye, Solving a system of fractional partial differential equations arising in the model of HIV infection of $CD4^+$ cells and attractor one-dimensional Keller-Segel equations, *Adv. Differ. Equ.*, 2013:94, 14 pages, (2013).
[14] F. Mainardi, Fractional relaxation-oscillation and fractional diffusion-wave phenomena, *Chaos Solit. Fract.* **7**, 1461–1477 (1996).
[15] D. Baleanu, About fractional quantization and fractional variational principles, *Commun. Nonlin. Sci.* **14**, 2520–2523 (2009).
[16] C.M.A. Pinto and J.A. Tenreiro Machado, Complex order van der Pol oscillator, *Nonlinear Dyn.* **65**(3), 247–254 (2010).
[17] C.M.A Pintoand J.A. Tenreiro Machado, Complex-order forced van der Pol oscillator, *J. Vibr. Contr.* **18**(14), 2201–2209 (2012).
[18] R. Nigmatullin and D. Baleanu, Is it possible to derive Newtonian equations of motion with memory?, *Int. J. Theor. Phys.* **49**, 701–708 (2010).

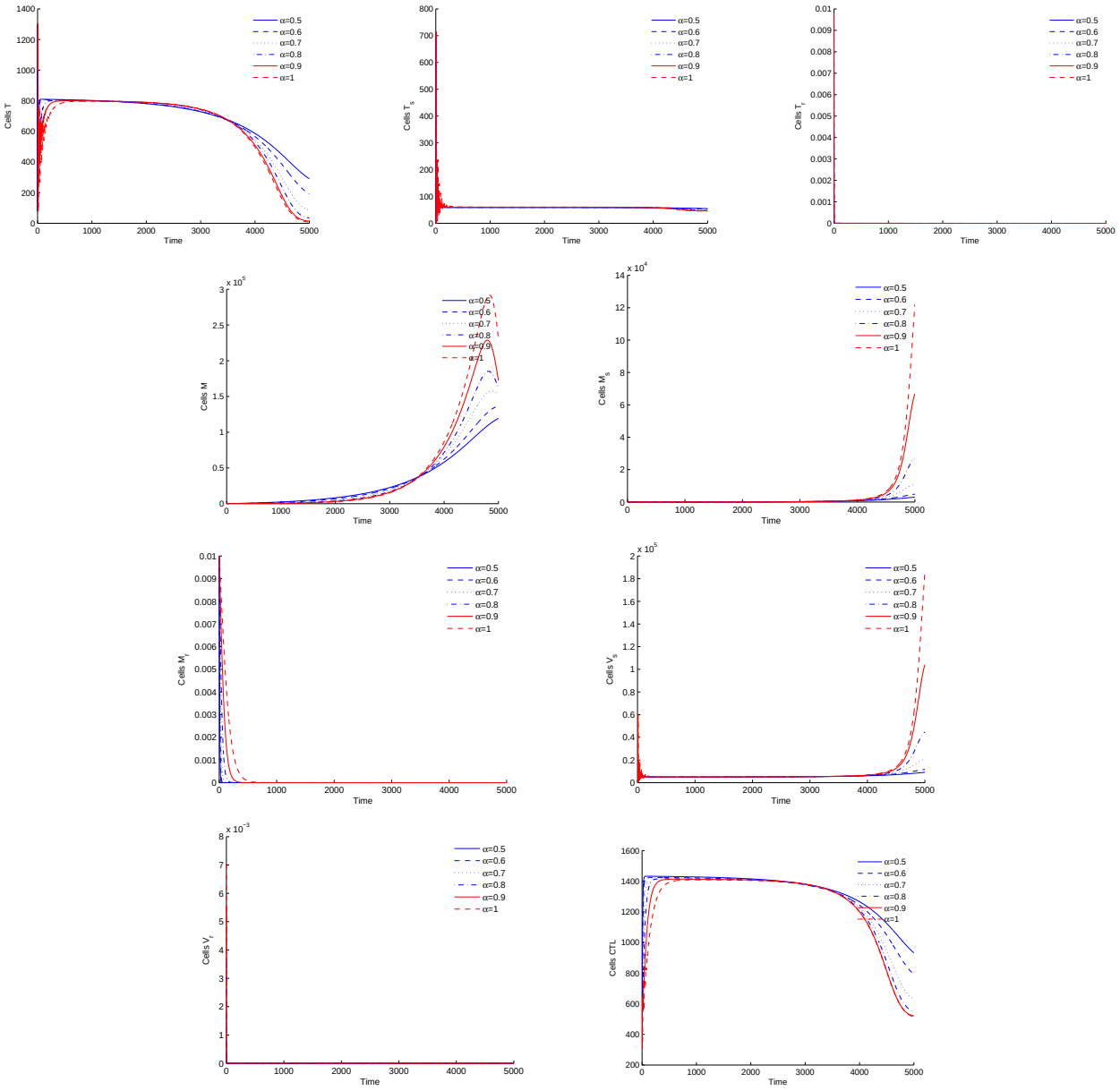

Fig. 4: Dynamics of the long term non-progressors of the fractional order model (3) for $\alpha \in \{0.5, 0.6, 0.7, 0.8, 0.9, 1.0\}$. Parameter values are those of Table 1 and initial conditions are given in the text.

[19] C.M.A Pinto and J.A Tenreiro Machado, Fractional model for malaria transmission under control strategies, *Comput. Math. Appl.* **66**, 908–916 (2013).

[20] C.M.A. Pinto and A.R.M. Carvalho, New findings on the dynamics of HIV and TB coinfection models, *Appl. Math. Comput.* **242**, 36–46 (2014).

[21] E. Ahmed, A.M.A. El-Sayed and H.A.A. El-Saka, On some Routh-Hurwitz conditions for fractional order differential equations and their applications in Lorenz, Rössler, Chua and Chen systems, *Phys. Lett. A* **358**, 1–4 (2006).

[22] Y. Wang, F. Brauer and J. Wu, J.M. Heffernan, A delay-dependent model with HIV drug resistance during therapy, *J. Math. Anal. Appl.* **414**, 514–531 (2014).

[23] R. Luo, M.J. Piovoso, J. Martinez-Picado and R. Zurakowski, HIV Model Parameter Estimates from Interruption Trial Data including Drug Efficacy and Reservoir Dynamics, *PLoS ONE* **7**, e40198 (2012).

[24] S.H. Bajaria, G. Webb, M. Cloyd and D. Kirschner, Dynamics of naive and memory $CD4^+$ T lymphocytes in HIV-1 disease progression, *J. AIDS* **30**, 41–58 (2002).
[25] S. LeBlanc, *The Long and the Short of AIDS Progression*, The Bay Area Report, 1996.
[26] M.J. Mugavero, S. Napravnik, S.R. Cole, J.J. Eron, B. Lau, H.M. Crane, M.M. Kitahata, J.H. Willig, R.D. Moore, S.G. Deeks and M.S. Saag, Viremia Copy-Years Predicts Mortality Among Treatment-Naive HIV-Infected Patients Initiating Antiretroviral Therapy, *Clin. Infect. Dis.* **53**(9), 927-935 (2011).